Chinese Chemical Letters 37 (2026) 111218

Contents lists available at ScienceDirect

Chinese Chemical Letters

journal homepage: www.elsevier.com/locate/cclet

An electrochemical immunosensor based on an antibody-ferrocene-functionalized covalent organic framework

Qiang Fang[a,b], Yingbo Lu[c], Jianying Huang[b], Cheng Zhang[a,*], Jing Wu[c], Shijun Li[c,*]

[a] College of Chemical Engineering, Zhejiang University of Technology, Hangzhou 310014, China
[b] College of Food Science and Biotechnology, Zhejiang Gongshang University, Hangzhou 310018, China
[c] College of Material, Chemistry and Chemical Engineering, Key Laboratory of Organosilicon Chemistry and Material Technology of Ministry of Education, Hangzhou Normal University, Hangzhou 311121, China

ARTICLE INFO

Article history:
Received 16 January 2025
Revised 9 April 2025
Accepted 15 April 2025
Available online 15 April 2025

Keywords:
Covalent organic frameworks
Post-functionalization
Ferrocene
Electrochemical immunosensors
Alpha-fetoprotein

ABSTRACT

High-sensitive quantitative determination of alpha-fetoprotein (AFP) is of crucial importance for early clinical diagnosis of cancers. Herein, an AuNPs-free electrochemical immunosensor (Ab1-Fc-COF) was prepared from a carboxylic group enriched COF by post-functionalization with detecting antibody (Ab1) and ferrocene (Fc), and used for electrochemical detection of AFP. Due to the small, homogeneous pore size of the COF, Ab1 with a big size was immobilized on the surface of the COF, while Fc with a small size was covalently modified both on the surface and in the pores of COF. The covalently immobilized Ab1 was quite stable and beneficial to specifically detect AFP biomarkers. Meanwhile, the enriched Fc molecules not only improved the conductivity of the COF, but also effectively transferred and amplified the electrochemical signal. This proposed immunosensor exhibited high sensitivity in detecting AFP with a detection limit of 0.39 pg/mL (S/N of 3:1) and a wide linear response range spanning from 1 pg/mL to 100 ng/mL when plotted against logarithmic concentrations. Furthermore, this immunosensor showed excellent selectivity, stability and reproducibility in the testing of real samples. This study presents an innovative prototype for construction of a precious metal-free, antibody-directly-immobilized, simple and stable electrochemical immunoprobe.

© 2025 Published by Elsevier B.V. on behalf of Chinese Chemical Society and Institute of Materia Medica, Chinese Academy of Medical Sciences.

Cancer is a multifaceted global health issue because of its serious lethality. The chances of survival can be substantially improved if cancer is detected at early stages to allow an appropriate timely therapy for preventing cancer development. As a consequence, early detection is very crucial for cancer treatment. Numerous and continuous efforts with interdisciplinary collaboration have been made to achieve early detection of cancers [1]. Alpha-fetoprotein (AFP) is a critical tumor marker, which indicates testicular, gastric or liver cancers at high levels [2,3]. Therefore, ultra-sensitive quantitative determination of AFP concentration in human plasma is of significant importance for early clinical diagnosis and treatment of cancers.

Up to now, a variety of methods for AFP detection have been developed, such as enzyme-linked immunosorbent assay (ELISA) [4,5], fluorescence immunoassay [6,7], chemiluminescence immunoassay [8], photoelectric immunoassay [9,10], as well as electrochemical immunoassay [11,12]. Among them, electrochemical immunoassay has attracted more attention due to its good selectivity, high sensitivity and rapid response [13–15]. The sensitivity of electrochemical immunosensors can be dramatically improved by electrochemical signal amplification, thus enabling early AFP detection [16]. In previous reports, nanozymes [17], nanomaterials [18] and cascade reactions [19] have been employed to amplify the electrochemical signals and enhance the sensitivity of electrochemical immunosensors. However, in these strategies, the electrochemical signals are usually not directly amplified. The methods with more effective and direct amplification of electrochemical signals are obviously advantageous and highly desired in early AFP detection [16,20].

Covalent organic frameworks (COFs), a kind of ordered crystalline organic porous materials connected by covalent bonds, have been extensively applied in gas adsorption [21,22], pollutant removal [23], catalysis [24], molecular recognition [25,26] and biomacromolecule fields [27,28]. The large loading capacity and specific surface area, diverse structures, good stability and remarkable adsorption properties of COFs make them considerable potential for the applications in biosensors [29–31]. Nevertheless, most COFs are lack of electroactivity, which limit their applications in

* Corresponding authors.
E-mail addresses: czhang@zjut.edu.cn (C. Zhang), l_shijun@hznu.edu.cn (S. Li).

https://doi.org/10.1016/j.cclet.2025.111218
1001-8417/© 2025 Published by Elsevier B.V. on behalf of Chinese Chemical Society and Institute of Materia Medica, Chinese Academy of Medical Sciences.

electrochemical detections. To solve this problem, the molecules with electroactivity [32–34] or catalytic activity [35,36] were used to functionalize COFs. For example, electroactive methylene blue was used to co-fabricate COF-based electrochemical sensors for prostate-specific antigen detection [37,38]. A COF was prepared from an electroactive precursor, thionine (Thi), and further modified with gold nanoparticles (AuNPs) for the application in electrochemical detection of carcinoembryonic antigen [39]. An iron-porphyrin COF based immunosandwich sensor with dual signal enhancement was fabricated for neuron-specific enolase immunodetection [40]. However, in spite of their great success for detection of biomolecules, these COFs-based electrochemical biosensors still suffered from a few shortcomings, including instability and poor reproducibility, especially when some COFs were used as supporting materials through hydrogen bonding and/or π–π stacking interactions due to lack of functional groups for directly covalent modification. Additionally, to tackle the poor inherent conductivity of COFs, amplify electrochemical signals and facilitate the immobilization of antibody, assembling AuNPs on the surface of COFs to form complex nanocomposites was usually necessary. However, this caused those probes fragile and expensive. Consequently, there is an urgent need to develop a stable and precious metal-free COF-based probe for electrochemical immunosensor applications.

Ferrocene (Fc) has unique electrochemical properties as an iconic redox marker [41,42]. The presence of abundant Fc molecules can remarkably enhance the conductivity of supporting materials [43,44], so it is a good choice to introduce Fc as an electrode constituent for electrochemical sensors. For example, Wang *et al*. prepared a Fc-contained COF (Fc-COFNs) for the detection of cardiac troponin I, where the introduction of Fc molecules overcame the poor electroactivity limitation of COFs [45]. Unfortunately, the aqueous stability of Fc-COFNs remains a challenge due to the fragile linkage of B–O bonds. Yang and coworkers reported the COF functionalized with ferrocene carboxylic acid (Fc-COOH), AuNPs, and complementary DNA probe (L1) to form the immunoprobe COF/Au/Fc/L1 for electrochemical determination of MicroRNAs [46]. However, the improvement of electrochemical signal by bonding Fc-COOH to the insufficient terminal amino groups on the COF was limited and meanwhile, to improve the conductivity of the COF, amplify electrochemical signals and immobilize antibody, AuNPs was also used. That is, the electrochemical probe is still a complex nanocomposite of using expensive gold nanoparticles.

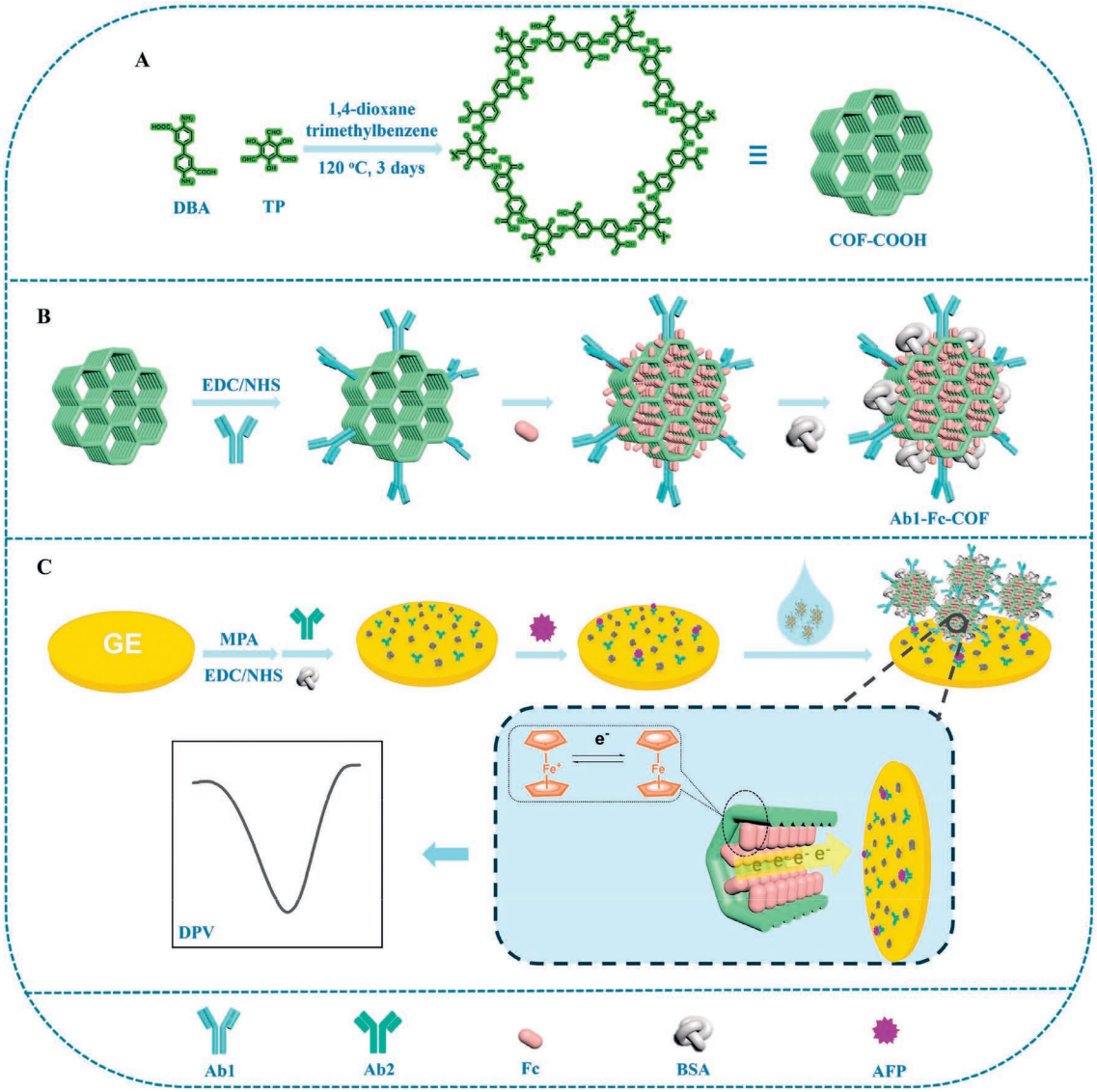
Herein, we designed a highly electroactive, gold nanoparticle-free, antibody-directly-immobilized electrochemical immunoprobe based on an Ab1-Fc-functionalized COF for sensitive detection of AFP. A carboxylic group-rich COF (COF-COOH) was synthesized and then covalently coupled with antibody (Ab1) and excessive ferrocene in sequence by using a simple, effective post-modification method to form the Ab1-Fc-COF (Schemes 1A and B), which was subsequently used as a novel electrochemical immunoprobe without AuNPs. In this immunoprobe, the suitable homogeneous pore size of the COF-COOH, which is smaller than Ab1 and larger than Fc, allows the Ab1 to be covalently decorated on the surface of COF, and enables the Fc to be modified in interior pores of the COF other than on the surface by reacting with the remained COOH. The interfacial Ab1 can be fully exposed to the antigen and beneficial to acquire good specificity. The abundant electrochemically active Fc in the ordered crystal structure of COF can not only improve the conductivity of COF but also significantly amplify electrochemical signal (Scheme 1C), resulting in a high electrochemical signal and excellent sensitivity with no use of gold nanoparticles. As expected, the proposed electrochemical immunosensor exhibited excellent analytical performance for AFP detection and was successfully applied in the analysis of practical samples.

The COF-COOH was synthesized from the precursors 2,4,6-triformylphloroglucinol (TP) and 4,4′-diamino-[1,1′-biphenyl]-3,3′-dicarboxylic acid (DBA) using acetic acid as a catalyst at 120 °C for 3 days in a mixed solvent of 1,4-dioxane/trimethylbenzene according to a similar previously reported procedure (Scheme 1A) [47]. The resulting COF-COOH was systematically characterized. The FT-IR spectrum (Fig. 1A) showed that the C=O bonds (1638 cm^{-1}) and C–H bonds (2899 cm^{-1}) of aldehydes in TP, as well as the N–H bonds (3380, 3497 cm^{-1}) in DBA were absent after the condensation, while new peaks appeared at 1702, 1575 and 1224 cm^{-1} attributing to the C=O, C=C and C–N bonds, respectively, indicative of the formation of keto-form structure in COF-COOH [48,49]. Meanwhile, the peaks at 184, 147, and 110 ppm in the ^{13}C solid-state nuclear magnetic resonance (SNMR) spectrum of COF-COOH further proved the presence of C=O, C–N, C=C bonds (Fig. S1 in Supporting information). The COF-COOH was then post-functionalized by Ab1 and excessive Fc-NH_2, successively. As it could be seen in the FT-IR spectrum, the absorption peak of C=O shifted from 1702 cm^{-1} to 1740 cm^{-1} with a decreased intensity and the peak of C–N shifted from 1224 cm^{-1} to 1236 cm^{-1} after post-functionalization. Additionally, a new peak at 489 cm^{-1} belonging to Fc was observed, which further confirmed successful functionalization [50].

The powder X-ray diffraction (PXRD) pattern of COF-COOH showed a highly intense peak at 3.4° corresponding to the (100) plane and an intense peak at 6.1° corresponding to the (110) plane (Fig. 1B). These planes closely matched the eclipsed AA-stacking model, which was characterized by a space group *P6/m* and lattice parameters of $a = b = 29.6$ Å, $c = 3.9$ Å, $\alpha = \beta = 90°$, and $\gamma = 120°$. The relevant R_{WP} and R_P values were 2.57 % and 1.85 %, respectively. The PXRD patterns of COF-COOH and Ab1-Fc-COF confirmed that the crystal structure was maintained after post-functionalization. The Brunauer-Emmett-Teller (BET) surface area of COF-COOH was determined to be 178 m^2/g (Fig. S2 in Supporting information), with a pore size distribution of 1.94 nm as calculated by fitting the nonlocal density functional theory (NLDFT). Obviously, this pore size is smaller than the molecular size of Ab1 but larger than that of Fc, which implies that Ab1 was modified only on the surface of COF allowing it to be fully exposed to the antigen and Fc was enriched both on the surface and in the pores of COF which amplified the electrochemical signal efficiently. After functionalization, the pores of COF were nearly filled with Fc, leading to the disappearance of pores and a significant reduction in BET surface area to 3 m^2/g (Fig. 1C).

The morphology of the materials was directly observed by scanning electron microscopy (SEM) and transmission electron microscopy (TEM). The synthesized COF-COOH displayed a rough, rod-like morphology with a diameter of approximately 100 nm and a length extending to several micrometers (Fig. 1D). The TEM image (Fig. 1F) revealed that the rough surface of COF-COOH was due to the presence of irregular protruding structures. After modification with Ab1 and Fc, the SEM image of Ab1-Fc-COF retained the rod-shaped morphology (Fig. 1E), though slight bending was observed. This deformation was possibly attributed to the introduction of Ab1 and Fc, which increased the interlayer spacing, consequently weakening the hydrogen bonding and/or π–π stacking interactions between the COF layers. The TEM image of Ab1-Fc-COF (Fig. 1G) showed relative decreases of both roughness and protrusions as compared with that of COF-COOH (Fig. 1F), which could be attributed to the surface modification with Ab1 and Fc.

To further confirm the successful functionalization, Ab1-Fc-COF was conducted to act with AF488-conjugated secondary antibody. Strong fluorescence of Ab1-Fc-COF was seen from confocal laser scanning microscopy (CLSM) (Fig. S3 in Supporting information), proving the successful decoration of Ab1 on the COF surface. Moreover, the abundant Fc loaded on the surface and interior of COF was directly observed in the elemental mapping of Ab1-Fc-COF, in



Scheme 1. The preparation of (A) COF-COOH and (B) Ab1-Fc-COF. (C) The operational procedure and mechanism of the electrochemical immunosensor for AFP detection.

which the elements C, N, O and Fe uniformly distributed throughout the rod-shaped structure of COF (Fig. S4 in Supporting information).

The as-prepared Ab1-Fc-COF was subsequently utilized as an immunoprobe for the detection of AFP. The processes of electrode modification and immunodetection (Scheme 1C, detailed procedures provided in Supporting information) were characterized using electrochemical impedance spectroscopy (EIS) and cyclic voltammetry (CV) techniques. Fig. 2A illustrated the electrochemical impedance of the bare gold electrode (curve a), which displayed low impedance due to the lack of hindrance to electron transfer. Upon 3-mercaptopropionic acid (MPA) modification, there was a significant increase in the impedance (curve b). The presence of capturing antibody (Ab2) on the electrode led to a larger semicircular arch in curve c as compared to curve b, confirming its successful binding. The loading of bovine serum albumin (BSA) further increased the electrochemical impedance (curve d), and a subsequent increase in impedance was observed after capturing AFP (curve e), indicating successful recognition of AFP. Furthermore, the immunobinding of Ab1-Fc-COF with AFP resulted in a continuous increase in impedance (curve f). Fig. 2B showed a corresponding decrease in peak current of CV curves. These results provided solid evidence for the successful assembly of the proposed electrochemical immunosensor.

The mechanism of signal amplification by Ab1 and Fc was subsequently investigated. As shown in Fig. 3A, a significant electrochemical signal was observed when Ab1-Fc-COF was utilized for AFP detection. Conversely, when Fc-functionalized COF (Fc-COF) was employed for AFP detection, a weak electrochemical signal was observed, attributed to non-specific adsorption. Notably, the utilization of Ab1-modified COF (Ab1-COF) resulted in complete absence of electrochemical signal. The results indicated that Ab1 served to identify AFP and fix Ab1-Fc-COF onto the electrode surface, while the enriched Fc groups generated and amplified electrochemical signal for quantitative detection of AFP. The signal amplification is mainly decided by the amount of Fc groups and the conductivity of functionalized COF. Thus, the conductivity of Ab1-Fc-COF was further studied. As shown in Fig. 3B, the impedance of Ab1-Fc-COF was obviously lower than that of Ab1-COF, indicating that the enriched Fc groups remarkably enhanced the conductivity of COF. The good conductivity can be owing to the excellent electroactivity of Fc and the favorable electron transfer in the nanochannels of COF which facilitates the electrochemical signal transmission from Fc to the electrode surface (Scheme 1C) [51].

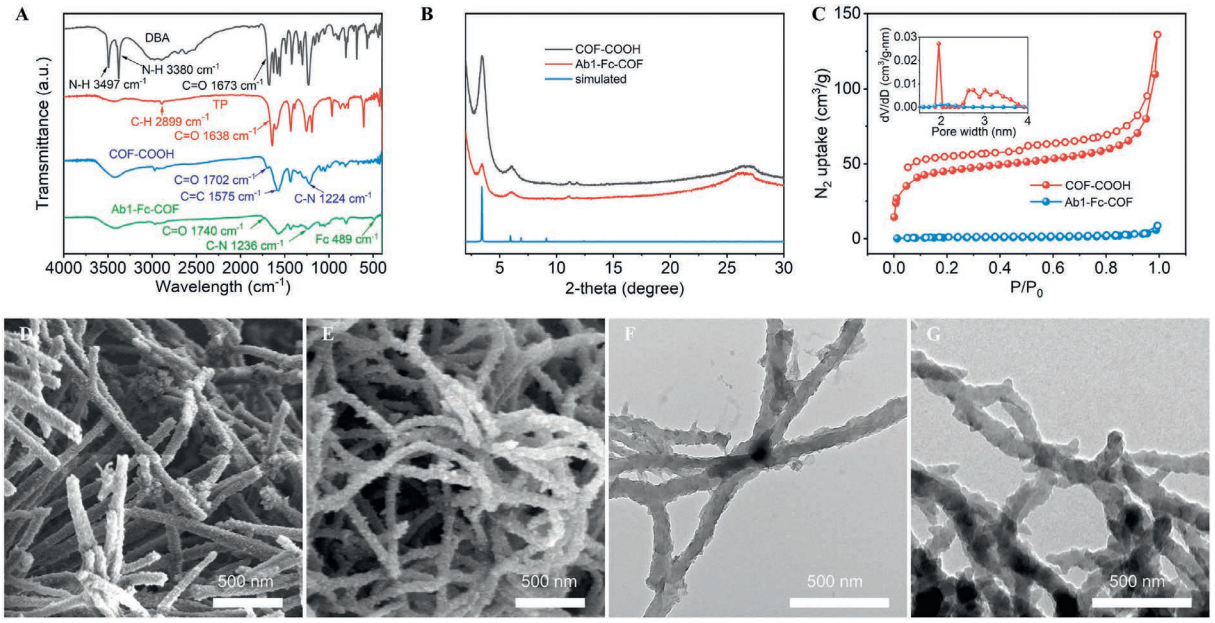


Fig. 1. (A) The FT-IR spectra of DBA, TP, COF-COOH and Ab1-Fc-COF. (B) The PXRD patterns of COF-COOH, Ab1-Fc-COF and simulated pattern of COF-COOH from the eclipsed AA-stacking mode. (C) N_2 adsorption-desorption isotherms and pore size distribution profiles (insert) of COF-COOH and Ab1-Fc-COF. SEM images of (D) COF-COOH and (E) Ab1-Fc-COF. TEM images of (F) COF-COOH and (G) Ab1-Fc-COF.

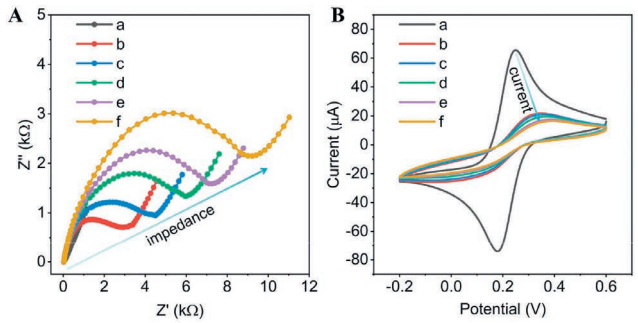


Fig. 2. Electrochemical characterization of electrode modification and immunodetection. (A) EIS and (B) CV of (a) bare GE, (b) MPA/GE, (c) Ab2/MPA/GE, (d) BSA/Ab2/MPA/GE, (e) AFP/BSA/Ab2/MPA/GE, and (f) Ab1-Fc-COF/AFP/BSA/Ab2/MPA/GE.

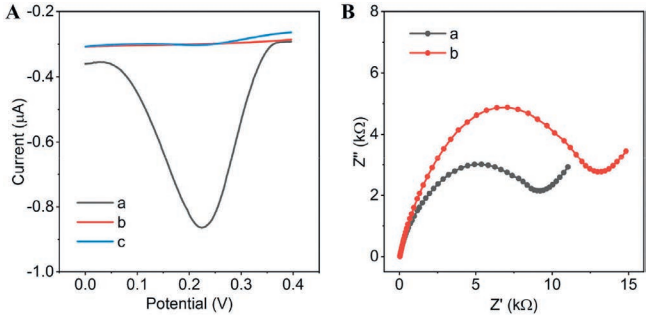


Fig. 3. (A) DPV of the immunosensors detecting 1 ng/mL AFP with (a) Ab1-Fc-COF, (b) Ab1-COF and (c) Fc-COF. (B) EIS of (a) Ab1-Fc-COF and (b) Ab1-COF.

To optimize the performance of the electrochemical immunosensor, the amount and incubation time of Ab1 and Fc in preparing Ab1-Fc-COF were investigated by detecting 1 ng/mL of AFP as a model. As illustrated in Fig. S5 (Supporting information), the maximum current responses were obtained when 0.4 mg/mL Fc and 10 μg/mL Ab1 were incubated at 4 °C with activated COF-COOH during 6 and 12 h, respectively. The recognition performance

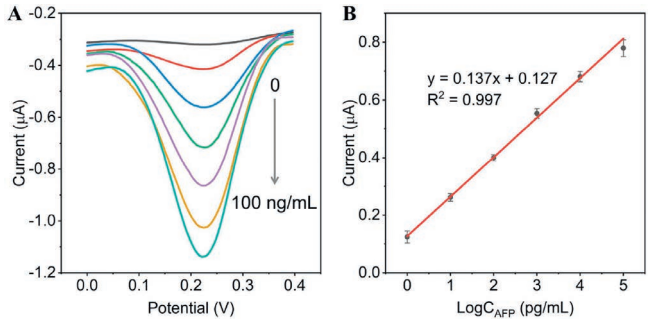


Fig. 4. (A) DPV of immunosensors incubated with various concentrations of AFP. (B) The corresponding calibration plot for AFP concentrations and DPV peak currents.

of Ab1-Fc-COF seldom increased or even decreased when a higher amount or longer incubation time of Fc and Ab1 were performed (Figs. S5A–D). On the other hand, the concentration and incubation time of Ab1-Fc-COF for detection of AFP were also optimized. As shown in Fig. S5E, the maximum value of the response peak current was acquired at a concentration of 0.2 mg/mL Ab1-Fc-COF, so it was selected as the optimized concentration of Ab1-Fc-COF. The current response increased with the prolongation of incubation time of Ab1-Fc-COF, and reached a satisfactory level after a 60-min incubation. Extending the incubation time beyond 60 min did not apparently enhance the current response. Therefore, 60 min was established as the optimal incubation time (Fig. S5F). As shown in Fig. S6 (Supporting information), the optimal concentration and incubation time of Ab2 for the electrode were 0.2 mg/mL and 12 h, respectively.

The analytical performance of the Ab1-Fc-COF was subsequently investigated for the detection of AFP under the optimized experimental conditions. The corresponding DPV curves that related to the concentrations of AFP were obtained. It was found that the peak currents of the immunosensor enhanced continuously as the concentrations of AFP increased (Fig. 4A). The detection limit of AFP was determined to be 0.39 pg/mL (S/N of 3:1). Furthermore, good linear relationship between the peak current and the log-

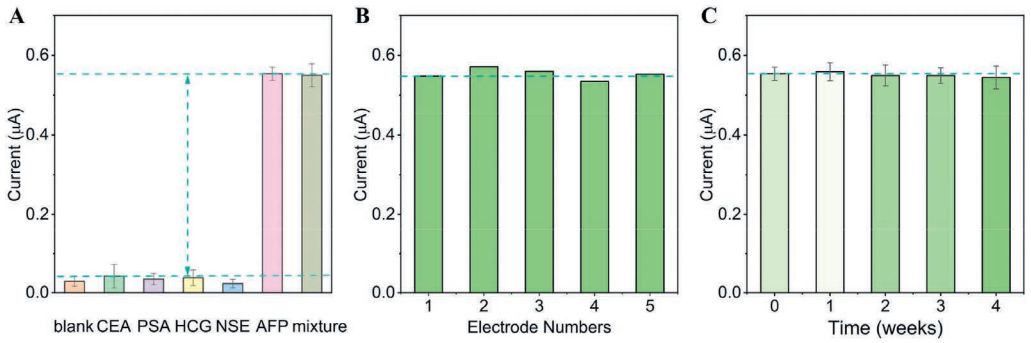


Fig. 5. (A) Selectivity evaluation of the immunosensor with AFP (1 ng/mL) and other antigens (10 ng/mL). (B) The reproducibility of the fabricated biosensor. (C) Stability of the immunosensor for detecting AFP (1 ng/mL) at an interval of one week.

arithm of AFP concentration, covering a range from 1 pg/mL to 100 ng/mL, was obtained with a high linear correlation coefficient of 0.997 (Fig. 4B). In comparison to other recently developed AFP detection immunosensors (Table S1 in Supporting information), this immunosensor with no use of gold nanoparticle exhibited comparable or even superior sensitivity and meanwhile had a relatively wide linear range thanks to the enriched Fc on and in the COF and Ab1 doped on the surface of COF.

The specificity of the immunosensor was then assessed by detecting other antigens, including carcinoembryonic antigen (CEA), prostate specific antigen (PSA), human chorionic gonadotropin (HCG) and neuron-specific enolase (NSE). The results in Fig. 5A revealed that the electrochemical signals for CEA (10 ng/mL), PSA (10 ng/mL), HCG (10 ng/mL) and NSE (10 ng/mL) were similar to that of the blank sample and significantly lower than that of the AFP (1 ng/mL) sample. In contrast, the electrochemical signal of a mixture containing AFP (1 ng/mL), CEA (10 ng/mL), PSA (10 ng/mL), HCG (10 ng/mL) and NSE (10 ng/mL) closely resembled that of the AFP sample. From these results, it can be concluded that the proposed immunosensor has excellent specificity.

Subsequently, five independent batches of immunosensors were repeatedly fabricated to detect AFP (1 ng/mL) under standard experimental conditions to evaluate the reproducibility of Ab1-Fc-COF. As shown in Fig. 5B, the relative standard deviation (RSD) value was 2.5 % ($n = 5$), indicative of a good reproducibility of the probe. The stability of the immunosensor was further evaluated by storing it at 4 °C for different durations. As shown in Fig. 5C, the immunosensor exhibited only a slight decrease in the electrochemical signal after 4 weeks, confirming its outstanding stability, which could be derived from the good stability of the Ab1-Fc-COF immunoprobe.

Furthermore, the practicality of this COF-based immunosensor was proven by analyzing real samples using the standard addition method (Table S2 in Supporting information). The samples with different concentrations of AFP in 10 % diluted human serum were prepared and each sample of diluted human serum was repeatedly measured three times (in triplicate). The results presented in Table S2 showed a recovery range of 95.7 % to 108.5 %, indicative of the good practicality and promising potential of this immunosensor for clinical applications in the analysis of actual biological samples.

In conclusion, a novel COF-based electrochemical immunoprobe Ab1-Fc-COF with excellent electrochemical properties and good stability, however without use of AuNPs, was successfully prepared by post-modification of a carboxylic acid-rich COF with Ab1 and Fc. Due to the small, homogeneous pore size of the COF, Ab1 was immobilized on the surface of the COF, which allowed it to be fully exposed to the antigen and exhibit good specificity for AFP detection. A large amount of Fc being covalently decorated on the surface and in the pores of the COF not only can improve the conductivity of the COF, which is beneficial to the transfer of the electrochemical signal from COF to the electrode, but also can directly amplify the electrochemical signal without use of AuNPs. Under optimal experimental conditions, the established electrochemical immunoprobe demonstrated excellent sensitivity with a detection limit of 0.39 pg/mL and a wide linear response range spanning from 1 pg/mL to 100 ng/mL. The covalent linking of Ab1 and Fc with the COF enabled its high stability, while the straightforward preparation process led to good reproducibility of the probe. Additionally, high recoveries were obtained in detection of AFP in real human serum samples, indicating its good practicality. Although this new immunosensor is highly effective and promising, considerable challenges still need to be overcome for implementing its large-scale clinical application, such as difficulties in large-scale preparation of COF-COOH at mild conditions. Efforts to solve the synthesis problem or find new porous materials will be made in the future in our labs to enable the application of this type of electrochemical immunoprobe in the large-scale clinical analysis of tumor markers.

Declaration of competing interest

The authors declare that they have no known competing financial interests or relationships that could have appeared to influence the work reported in this paper.

CRediT authorship contribution statement

Qiang Fang: Writing – original draft, Investigation. **Yingbo Lu:** Writing – review & editing, Investigation. **Jianying Huang:** Resources, Methodology. **Cheng Zhang:** Writing – review & editing, Supervision. **Jing Wu:** Validation, Methodology. **Shijun Li:** Writing – review & editing, Supervision, Funding acquisition, Conceptualization.

Acknowledgments

We thank the Natural Science Foundation of Zhejiang Province (No. LZ24B020005) and the National Natural Science Foundation of China (No. 22071040) for financial support.

Supplementary materials

Supplementary material associated with this article can be found, in the online version, at doi:10.1016/j.cclet.2025.111218.

References

[1] D. Crosby, S. Bhatia, K.M. Brindle, et al., Science 375 (2022) eaay9040.

[2] N. Tayob, F. Kanwal, A. Alsarraj, et al., Clin. Gastroenterol. Hepatol. 21 (2023) 415–423.
[3] Z.H. Yang, J. Yin, L. Xin, et al., Chin. Chem. Lett. 35 (2024) 109558.
[4] H. Moulahoum, F. Ghorbanizamani, S. Timur, Anal. Chim. Acta 1306 (2024) 342617.
[5] S. Tang, J. Cai, K. Zhou, Anal. Methods 16 (2024) 6443–6450.
[6] C. Zheng, P. Dai, H. You, et al., Anal. Sci. 40 (2024) 1239–1248.
[7] Z. Song, Q. Hao, B. Li, et al., Chin. Chem. Lett. 36 (2025) 109834.
[8] B. Cong, W. Liang, W. Lai, et al., Bioelectrochemistry 156 (2024) 108626.
[9] H. Wu, X. Yang, Bioelectrochemistry 160 (2024) 108773.
[10] W. Chen, X. Zhang, M. Chi, et al., Anal. Chim. Acta 1330 (2024) 343281.
[11] Z. Shang, T. Su, D. Jin, et al., Biosens. Bioelectron. 230 (2023) 115245.
[12] F.B. Kayani, S. Rafique, R. Akram, et al., Nanotechnology 34 (2023) 265501.
[13] V.N. Palakollu, Y.V.M. Reddy, M.I. Shekh, et al., Clin. Chim. Acta 557 (2024) 117882.
[14] K. Malecka-Baturo, I. Grabowska, Talanta 281 (2025) 126870.
[15] S. Madhurantakam, B.E. David, A. Naqvi, et al., Anal. Methods 16 (2024) 6615–6633.
[16] C.W. Shan, Z. Chen, G.C. Han, et al., Talanta 271 (2024) 125638.
[17] D. Liang, Y. Wang, K. Qian, Interdiscip. Med. 1 (2023) e20230020.
[18] A.V.P. Patil, Y.S. Chuang, C. Li, et al., Biosensors 13 (2023) 125.
[19] Y. Zhu, Z. Cheng, X. Wang, et al., Biosens. Bioelectron. 274 (2025) 117222.
[20] M.S. Raziyan, A. Palevicius, G. Janusas, J. Electrochem. Soc. 171 (2024) 077510.
[21] J. Li, G. Chen, C. Chen, et al., Chin. Chem. Lett. 36 (2025) 109760.
[22] H. Li, Z. Zhou, T. Ma, et al., J. Am. Chem. Soc. 146 (2024) 35486–35492.
[23] X. Cao, Y. Jin, H. Wang, et al., Chin. Chem. Lett. 35 (2024) 109201.
[24] Z. Alsudairy, N. Brown, A. Campbell, et al., Mater. Chem. Front. 7 (2023) 3298–3331.
[25] Y. Chen, S. Huang, L. Xia, et al., Anal. Chem. 96 (2024) 1380–1389.
[26] C. Liu, C. Jia, S.X. Gan, et al., Chin. Chem. Lett. 35 (2024) 109750.
[27] W. Feng, C. Gao, R. Xu, et al., Coord. Chem. Rev. 515 (2024) 215965.
[28] Y. Shi, J. Yang, F. Gao, et al., ACS Nano 17 (2023) 1879–1905.
[29] F. Hernández-García, G.A. Álvarez-Romero, R. Colorado-Peralta, et al., J. Electrochem. Soc. 171 (2024) 077521.
[30] R. Xue, Y.S. Liu, S.L. Huang, et al., ACS Sens. 8 (2023) 2124–2148.
[31] E. Martínez-Periñán, M. Martínez-Fernández, J.L. Segura, et al., Sensors 22 (2022) 4758.
[32] C. Hou, J. Liu, S. Zhang, et al., Sens. Actuators B 417 (2024) 136221.
[33] S.H. Wen, H. Zhang, S. Yu, et al., Anal. Chem. 95 (2023) 14914–14924.
[34] S. Liu, Q. Zhang, X. Zhang, et al., Anal. Chem. 96 (2024) 10408–10415.
[35] X. Peng, J. Zhu, Z. Wu, et al., Sens. Actuators B 392 (2023) 134074.
[36] M. Wang, Y. Pan, S. Wu, et al., Biosens. Bioelectron. 169 (2020) 112638.
[37] J. Zheng, H. Zhao, G. Ning, et al., Talanta 233 (2021) 122520.
[38] H. Liang, H. Xu, Y. Zhao, et al., Biosens. Bioelectron. 144 (2019) 111691.
[39] H. Liang, Y. Luo, Y. Li, et al., Anal. Chem. 94 (2022) 5352–5358.
[40] H. Liang, Y. Luo, Y. Xiao, et al., Chem. Eng. J. 460 (2023) 141740.
[41] H. Beitollahi, M.A. Khalilzadeh, S. Tajik, et al., ACS Omega 5 (2020) 2049–2059.
[42] G. Roy, R. Gupta, S.R. Sahoo, et al., Coord. Chem. Rev. 473 (2022) 214816.
[43] M. Dervisevic, E. Dervisevic, M. Senel, et al., Enzyme. Microb. Tech. 102 (2017) 53–59.
[44] R.E. Ruther, Q. Cui, R.J. Hamers, et al., J. Am. Chem. Soc. 135 (2013) 5751–5761.
[45] Z. Song, J. Song, F. Gao, et al., Sens. Actuators B 368 (2022) 132205.
[46] S. Feng, Y. Xue, J. Huang, et al., Anal. Chem. 94 (2022) 16945–16952.
[47] J.Y. Yue, L. Wang, Y. Ma, et al., Dalton Trans. 48 (2019) 17763–17769.
[48] S. Kandambeth, A. Mallick, B. Lukose, et al., J. Am. Chem. Soc. 134 (2012) 19524–19527.
[49] B.P. Biswal, S. Chandra, S. Kandambeth, et al., J. Am. Chem. Soc. 135 (2013) 5328–5331.
[50] T. Feng, X. Qiao, H. Wang, et al., Biosens. Bioelectron. 79 (2016) 48–54.
[51] Y. Cao, R. Wu, Y.Y. Gao, et al., Nano Micro Lett. 16 (2024) 37.